photonics

MDPI

Article

Advances in Optical Metrology: High-Bandwidth Digital Holography for Transparent Objects Analysis

Manoj Kumar [1,*], Lavlesh Pensia [2,3], Karmjit Kaur [4], Raj Kumar [2,3], Yasuhiro Awatsuji [5] and Osamu Matoba [6,7]

1 Amity School of Physical Sciences, Amity University Punjab, Sector 82A, Mohali 140306, India
2 CSIR-Central Scientific Instruments Organisation, Sector 30 C, Chandigarh 160030, India
3 Academy of Scientific and Innovative Research (AcSIR), Ghaziabad 201002, India
4 Government P.G. College Ambala Cantt, Ambala Sadar 133001, India
5 Faculty of Electrical Engineering and Electronics, Kyoto Institute of Technology, Matsugasaki, Sakyo-ku, Kyoto 606-8585, Japan
6 Department of Systems Science, Graduate School of System Informatics, Kobe University, Rokkodai 1-1, Nada, Kobe 657-8501, Japan
7 Center of Optical Scattering Image Science, Kobe University, Rokkodai 1-1, Nada, Kobe 657-8501, Japan
* Correspondence: manojklakra@gmail.com or mkumar@pb.amity.edu

Abstract: Accurate and non-invasive optical metrology of transparent objects is essential in several commercial and research applications, from fluid dynamics to biomedical imaging. In this work, a digital holography approach for thickness measurement of glass plate and temperature mapping of candle flame is presented that leverages a double-field-of-view (FOV) configuration combined with high spatial bandwidth utilization (SBU). By capturing a multiplexed hologram from two distinct objects in a single shot, the system overcomes the limitations inherent to single-view holography, enabling more comprehensive object information of thickness measurement and temperature-induced refractive index variations. The method integrates double-FOV digital holography with high SBU, allowing for accurate surface profiling and mapping of complex optical path length changes caused by temperature gradients. The technique exhibits strong potential for applications in the glass industry and microfluidic thermometry, convection analysis, and combustion diagnostics, where precise thermal field measurements are crucial. This study introduces an efficient holographic framework that advances the capabilities of non-contact measurement applications by integrating double-FOV acquisition into a single shot with enhanced spatial bandwidth exploitation. The approach sets the groundwork for real-time, volumetric thermal imaging and expands the applicability of digital holography in both research and industrial settings.

Keywords: digital holography; space bandwidth utilization; double-field-of-view; surface profiling; 3D temperature measurement

check for updates

Received: 15 May 2025
Revised: 12 June 2025
Accepted: 16 June 2025
Published: 18 June 2025

Citation: Kumar, M.; Pensia, L.; Kaur, K.; Kumar, R.; Awatsuji, Y.; Matoba, O. Advances in Optical Metrology: High-Bandwidth Digital Holography for Transparent Objects Analysis. *Photonics* **2025**, *12*, 617. https://doi.org/10.3390/photonics12060617

Copyright: © 2025 by the authors. Licensee MDPI, Basel, Switzerland. This article is an open access article distributed under the terms and conditions of the Creative Commons Attribution (CC BY) license (https://creativecommons.org/licenses/by/4.0/).

1. Introduction

Precise, non-invasive, and three-dimensional optical measurement is critical across a wide range of scientific and engineering disciplines, including thermal management in microfluidic devices [1], diagnostics in combustion systems [2], and biomedical imaging [3]. Precise thickness and surface profiling of transparent and semi-transparent materials is critical for quality control, material characterization, and performance optimization across several applications [4–7]. Traditional contact-based methods, including micrometer, caliper, and contact profilometer for thickness measurement for a thin transparent

film and thermocouples or resistance temperature detectors (RTDs) [8] for temperature measurement, often disrupt the surface/thermal field they aim to measure and do not provide full-field information and are limited by spatial resolution and response time. These methods are often unsuitable for environments with rapid temporal or spatial temperature fluctuations [8]. Consequently, there has been a growing demand for non-invasive optical techniques capable of measuring physical parameters with high accuracy, resolution, and temporal fidelity.

Among the non-invasive techniques for temperature measurement, infrared (IR) thermography has gained prominence due to its ease of use and capability for real-time surface temperature monitoring [9]. However, IR thermography is inherently limited to surface measurements and is sensitive to emissivity variations and environmental interferences. Optical interferometric techniques offer full-field and three-dimensional measurements, high resolution, and extremely high sensitivity to refractive index changes induced by temperature gradients [10]. Digital holography [11,12] has developed as a strong instrument for non-contact, full-field measurement of physical parameters, including thickness, deformation, displacement, vibration, refractive index, and temperature, because of its ability to record both the amplitude and phase of a light field in a single exposure. The phase information encodes optical path length changes, which are related to refractive index variations caused by temperature gradients in a transparent or semi-transparent medium. Despite its advantages, the technique faces several limitations; typically, it requires highly stable environmental conditions, complex optical alignments, and a limited field of view (FOV), therefore limiting its applicability in dynamic or field environments. The limited FOV is one of the inherent limitations of digital holography, primarily dictated by the trade-off between spatial resolution and detector size. Since digital holography relies on recording interference fringes on a pixelated sensor array, the maximum recoverable field is limited by the pixel pitch and the total number of pixels available [13]. A general expression for the FOV can be derived considering the relationship between the sensor dimensions, pixel size, and the magnification factor, as

$$FOV = \frac{sensor\ width \times pixel\ size}{magnification} \tag{1}$$

Consequently, conventional digital holography systems often face a performance bottleneck where achieving both high resolution and wide FOV simultaneously becomes challenging. These limitations are particularly problematic for applications such as full-field thickness profiling, deformation, displacement, vibration, refractive index measurement, temperature mapping, large-scale biological imaging, and industrial inspection, where both high-resolution and wide-area coverage are essential.

However, several strategies have been proposed and developed to address the limited FOV in digital holography. Some of these methods are multi-view projection holography [14,15], synthetic aperture digital holography [16], multiplexed digital holography [17–33], computational methods [34,35], lens-based digital holography [36,37], etc. In multi-view projection holography [14], the 2D images of a 3D object are recorded from various perspective points of view either by sequentially moving the object or the image sensor, and then they are digitally processed to yield a digital hologram. Another method [15] involves capturing holograms from multiple angles by moving the object or the image sensor and stitching these together to achieve a larger FOV without sacrificing resolution. These approaches require expensive mechanical equipment and time-consuming computations, making them unsuitable for investigating quick transient events. In synthetic aperture techniques [16], holograms are captured at different positions, and the Fourier spectra are combined to effectively "synthesize" a larger aperture, extending both resolu-

tion and FOV beyond the physical sensor limits. Synthetic aperture digital holography can achieve ultra-high-resolution imaging, though it typically requires mechanical scanning or precise stage control. Lens-based methods [13,37] for increasing the FOV require certain parameters such as focal length, location, and diameters, resulting in increased aberrations and making a bulkier system configuration.

In multiplexed approaches, several wavefronts, often from different angles or wavelengths, are encoded onto a single hologram by careful carrier frequency design. This enables the simultaneous recovery of multiple fields, effectively expanding the observable FOV without increasing acquisition time. The multiplexing approaches for extending the FOVs in digital holography require specialized and expensive optical components such as retro-reflectors [20], multiple mirrors [22,23], grating [23,24], Fresnel biprism [25], Fresnel bimirror [26], multifunctional holographic optical element [29], etc. These approaches require stringent requirements and the optical layout is complex and bulky. Therefore, there is a need to overcome the existing limitations of these systems by employing a simple and inexpensive optical component and simultaneously making the system layout simple. Continued improvements in detector technology, computational power, optical system design, and AI-based technologies [38] are expected to further bridge the gap between high-resolution, wide-FOV imaging and real-time, robust holographic measurement for complex, dynamic systems such as turbulent thermal fields and biological tissues.

In this work, we experimentally demonstrated the application of a recently developed double-FOV holographic system [27] by our group for enhanced imaging, thickness measurement of a glass plate, and phase mapping of a candle flame. A major advantage of the system is its simple optical layout, which uses a straightforward and affordable optical component (i.e., a cube beam splitter), making it superior to the other multiplexing approaches [18–33]. By simultaneously capturing holographic information from two distinct flames in a single-shot acquisition, we significantly increase the system's information capacity and spatial frequency coverage, resulting in improved object information characterization. The incorporation of high SBU ensures that the captured data fully exploits the available spatial frequencies, maximizing the effective resolution without necessitating complex optical setups or extensive computational post-processing. Thickness measurement and surface profiling are essential for quality control, performance optimization, and material characterization in advanced manufacturing and research. They ensure precision and reliability in applications ranging from thin films to photonic and biomedical devices. Similarly, for quality control in a variety of industries, including plastic, automotive, food, ceramics, and textiles, temperature measurement and optimization are essential. Optical methods are more appropriate and have been extensively employed for non-invasive deformation, surface profiling, refractive index, and temperature measurements by exploiting the dependence of phase. The non-contact techniques enable accurate characterization of transparent or delicate materials without physical interference, making them ideal for thin films, coatings, and photonic devices. Optical methods offer high resolution, speed, and repeatability, supporting innovation and reliability across industries such as semiconductors, optics, biomedical engineering, and materials science. Phase can be visualized optically via the Schlieren method and shadowgraph [39]. Although these methods are effective for visualizing the phase object, quantitative measurement of phases is difficult. Various optical methods, including holographic interferometry [40–42], Moiré deflectometry [43], laser speckle photography [44], shearing interferometry [45,46], speckle interferometry [47], digital holographic interferometry [48–52], etc., are commonly employed to measure phase or phase difference and associated parameters such as deformation, displacement, strain, refractive index, density, and temperature. Digital holography-based optical methods for optical metrology are more appropriate than other optical methods because they are easier

to implement, faster in operation, more resilient, and more precise and accurate. However, the limited FOV of the digital holographic systems is one of the major issues. Recently, we have developed a single-shot double-FOV digital holographic approach for biomedical applications. In this work, the developed single-shot digital holographic system is verified for a scientific or industrial application by measuring the thickness of the glass plate and phase distribution of candle flame.

This paper details the experimental setup and phase reconstruction methodology for the proposed system. Furthermore, the experimental results demonstrate its capability to achieve high-fidelity thickness measurement and phase mapping of candle flame. This multiplexing digital holographic approach provides a scalable, robust, and versatile solution for advanced optical metrology applications, extending the frontiers of digital holography-based surface profiling and temperature sensing.

2. Materials and Methods

Figure 1 depicts the experimental setup of the single-shot double-FOV digital holographic system. A He-Ne laser is used as the light source, which is spatially filtered by a spatial filter assembly with a microscope objective of 40× and a pinhole of 5 µm. This spatially filtered laser light is collimated by a lens with a focal length of 100 mm and a diameter of 50 mm. The collimated light beam is divided into two beams: the object and reference, by using a cube beam splitter (BS_1). The object beam of diameter ∼50 mm is passed through two objects (say Object 1 and Object 2) placed side-by-side. The object light transmitted through these objects is then allowed to pass through a cube beam splitter (BS_2) oriented at ∼ 45° w.r.t. the optical axis. The object diffraction wavefields corresponding to the two objects are allowed to pass through the two different prisms of BS_2. The diffracted object wavefield corresponding to Object 1 is 50% transmitted and 50% reflected through BS_2, and the same happened for the diffracted object wavefield corresponding to Object 2. Therefore, two sets of overlapped object wavefields corresponding to Object 1 and Object 2 are obtained at the exit of the BS_2. One set of these overlapped object wavefields is incident on the active region of the image sensor, whereas the other is blocked. This overlapped object wavefield carrying the object information of both objects is then allowed to interfere with the reference beam. This interference is accomplished by introducing another beam splitter (BS_3) in between BS_2 and the image sensor. Therefore, a multiplexed digital hologram is recorded by the digital image sensor carrying the two-object information in the single recorded hologram. The image sensor used in the experiment is a Sony Pregius IMX 249 model with a pixel number of 1920 × 1200 and a pixel size of 5.86 µm.

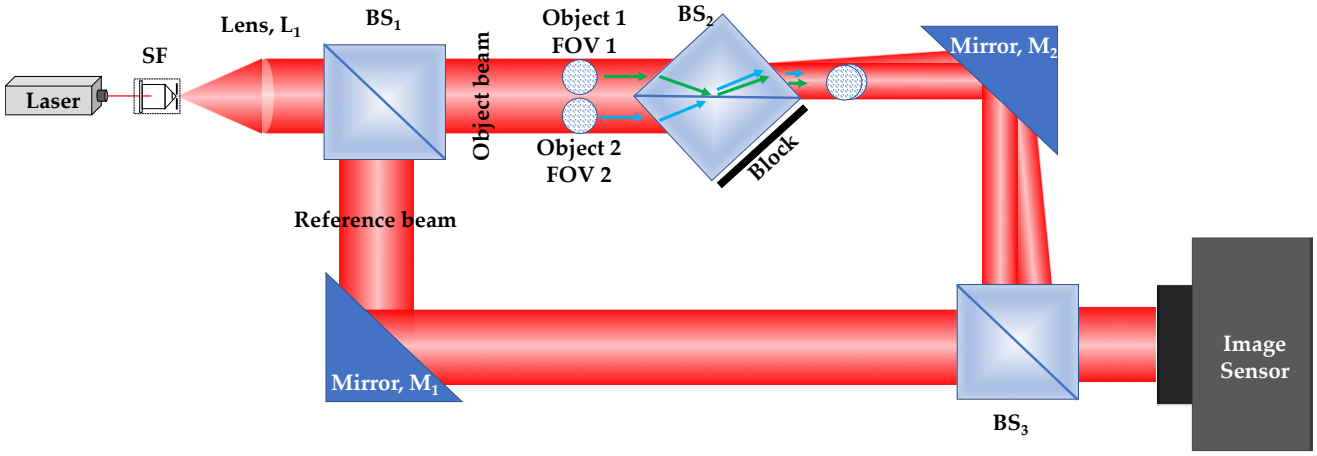


Figure 1. Schematic of the single-shot double-FOV digital holography.

In the holographic multiplexing approach, a single exposure allows for comprehensive reconstruction of the complicated wavefront. There is no overlap between the AC spectrum and conjugation spectra in the multichannel wavefronts' spatial spectra. Therefore, the sensor's redundant space bandwidth enhances spatial bandwidth utilization (SBU). The SBU is defined by $2\pi\Delta x^2(B_0/2)^2$, where B_0 is the bandwidth of the object wavefield and Δx is the pixel size of the image sensor. The digital hologram took up $M \times N$ pixels in the spatial frequency domain. Each conjugate term has a bandwidth B_0 of $M/4$ in the horizontal direction and $N/4$ in the vertical direction. Its area is $\pi(M/8) \times (N/8)$. In this work, the multiplex hologram uses $4\pi\,(MN/64)/MN$ = 19.63% of the bandwidth. On the other hand, a conventional off-axis digital holography has only 16.1% SBU [35], which ultimately results in a restricted imaging FOV using the same NA. However, a spectrum usage limit of 58.9% is possible due to the multiplexing limit of six channels in a single off-axis multiplexing hologram [20], but at the cost of a very complex system configuration. Recently, Huang and Cao [35] have reported an off-axis multiplexing digital holographic system by incorporating the Kramers–Kronig relation to allow for the overlapping between the signal spectra and unwanted spectra. This approach further enhances the bandwidth utilization of the sensor in a diffraction-limited optical system to 78.5% in one hologram.

3. Results

First, the experiment is performed on a United States Air Force (USAF) resolution target, in order to optimize the associated parameters of the holographic system and verify its double-FOV imaging capability. The USAF resolution target (Edmund Optics, USAF 1951 1X) and Thorlabs test target R1L3S2P are placed side-by-side in the object wavefield, and a multiplexed digital hologram is recorded, which carries the object information corresponding to these two FOVs of the resolution target. Figure 2a shows the recorded multiplexed digital hologram and Figure 2(a1) shows the enlarged view of the selected region of Figure 2a in red box. The intensity distribution of the multiplexed digital hologram is represented by

$$\begin{gathered} I(x,y) = \left|I(x,y)_{01} + I(x,y)_{02} + I_r\right|^2 \\ = \left|I(x,y)_{01}\right|^2 + \left|I(x,y)_{02}\right|^2 + \left|I(x,y)_r\right|^2 + I(x,y)_{01}I(x,y)^*_{02} \\ + I(x,y)_{02}I(x,y)^*_{01} + I(x,y)_{01}I(x,y)^*_r + I(x,y)_{02}I(x,y)^*_r \\ + I(x,y)_rI(x,y)^*_{01} + I(x,y)_rI(x,y)^*_{02} \end{gathered} \tag{2}$$

where $I(x,y)_{01}$ and $I(x,y)_{02}$ represent, respectively, the complex amplitude of the object beams for the two FOVs and $I(x,y)_r$ represents the reference beam. * represents the complex conjugation.

In Equation (2), the first three terms correspond to the auto-correlation (AC) term, whereas the other six terms contribute to the cross-correlation (CC) terms, as depicted in the Fourier spectrum of the multiplexed digital hologram in Figure 2b. The frequency radii of the AC and CC terms in the spectral domain of the hologram are represented by $2B$ and B, respectively, where $B = k\frac{NA}{\alpha M}$, with $k = \frac{2\pi}{\lambda}$, NA is the numerical aperture, M is the magnification, and α is the resolution criterion factor (Abbe's criterion). The modulation frequency needs to be greater than $3B$ in order to avoid information aliasing between AC and CC. The proposed approach shows a similar power spectrum of a diagonal off-axis multiplexing, as illustrated in Figure 2(c) of Ref. [53], and possesses the same bandwidth calculations.

The complex amplitudes (amplitude and phase) are obtained corresponding to the two FOVs by spatially filtering the CC terms $I(x,y)_{01}I(x,y)^*_r$ and $I(x,y)_{02}I(x,y)^*_r$ by following the Fresnel diffraction reconstruction method [11]. The retrieved amplitude

distribution corresponding to the two FOVs are shown in Figures 2a and 2b, respectively, and Figure 2e,f show their corresponding phase distributions.

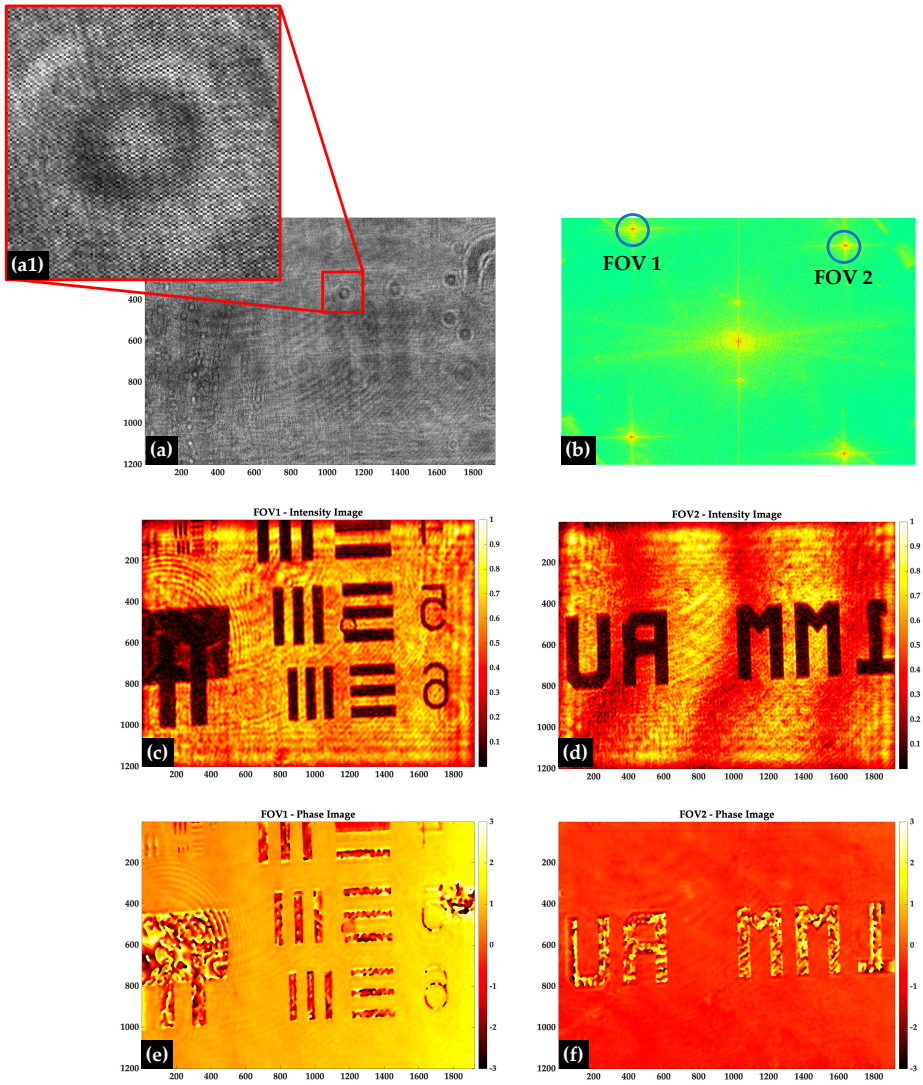


Figure 2. Experimental results of resolution target: (**a**) the recorded multiplexed digital hologram; (**a1**) the enlarged view of the selected region of (**a**) in red box which shows the multiplexed fringes; (**b**) Fourier spectrum of (**a**); (**c**,**d**) amplitude distributions corresponding to the two FOVs; and (**e**,**f**) phase distributions corresponding to the two FOVs.

In the next experiment, a step object is created by two glass plates (of dimensions $76 \times 26 \times 1$ mm^3) by placing one onto the other, and then this step object is placed in the entire object beam and two multiplexed digital holograms are recorded: one in the presence of the glass plate (object hologram) and another in the absence of the glass plate (reference hologram). The multiplexed digital hologram carries the complex amplitude information of two objects at the same time in a single-shot acquisition. Both the object and reference holograms are processed to obtain the phase distributions ($\Delta\phi_{obj}$ and $\Delta\phi_{ref}$). The phase distribution corresponding to the reference hologram ($\Delta\phi_{ref}$) is subtracted from the phase distribution of the object hologram ($\Delta\phi_{obj}$) to obtain the phase difference information ($\Delta\phi = \Delta\phi_{obj} - \Delta\phi_{ref}$). This phase difference is wrapped in the range ($-\pi$, $+\pi$) radian and it may range over an interval greater than 2π radians. This 2π phase discontinuity is removed by employing the PUMA phase unwrapping algorithm [54]. Finally, thickness

is measured by using the relationship between the obtained phase difference and the thickness, $t(x, y)$, as

$$\Delta\phi(x, y) = \frac{2\pi}{\lambda}\Delta n \times t(x, y) \tag{3}$$

where λ is the wavelength of the light source used and Δn is the refractive index difference between the object and the surrounding medium.

The obtained phase difference distributions corresponding to the two FOVs are depicted in Figures 3a and 3b, respectively. The measured thickness profiles from the obtained phase distributions by using Equation (2) corresponding to the two FOVs are shown in Figure 3c,d.

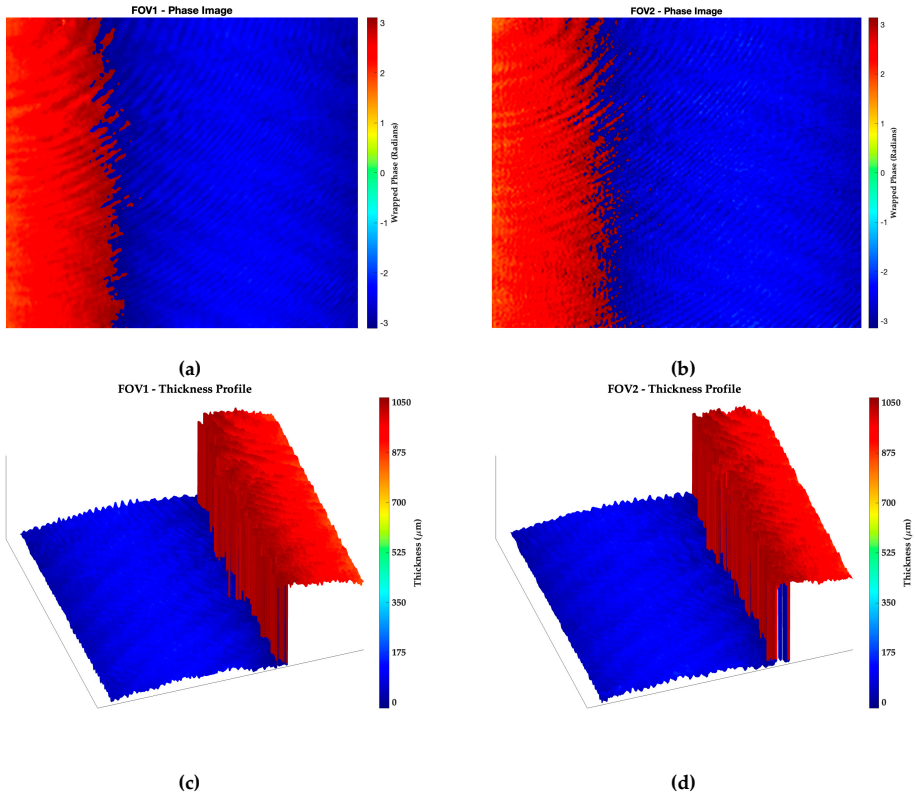


Figure 3. Experimental results of glass plate: (**a**,**b**) the retrieved wrapped phase distribution corresponding to the two FOVs, respectively; (**c**,**d**) thickness profile of the glass plate corresponding to the two FOVs.

Further, an experiment is performed for the dynamic phase visualization of two candle flames, where two multiplexed digital holograms are recorded: one in the presence of the candle flames and another without the candle flames. These two multiplexed holograms are processed and phase difference distributions corresponding to the two FOVs are obtained. The phase difference distributions for the two FOVs are depicted in Figures 4a and 4b, respectively. The obtained phase distributions corresponding to the two FOVs can further be used for the measurements of refractive index and temperature, similar to our previous works [50–52], by using the following mathematical expressions for refractive index and temperature connected to the obtained phase distribution:

$$\Delta\phi_i(x, y) = \int_{-z_0}^{z_0} \frac{2\pi}{\lambda}\Delta n(r, y)dz \tag{4}$$

$$n(r, y) = n_0 + \frac{\lambda}{2\pi}\int_r^R \left[\frac{d\{\Delta\phi(x, y)\}}{dx}\right]\frac{dx}{\sqrt{x^2 - r^2}} \tag{5}$$

where n_0 is the refractive index of air and $r = \sqrt{x^2 + z^2}$.

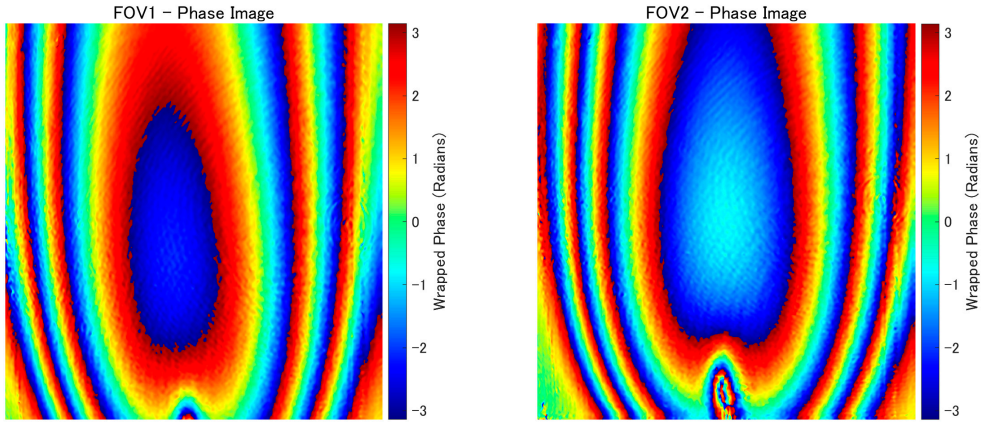


Figure 4. Experimental results of candle flame: (**a**,**b**) the retrieved wrapped phase distribution corresponding to the two FOVs, respectively.

4. Discussion

Digital holography has been proven to be a powerful imaging and measurement technique. The field has enormous potential to extend its usability in several applications by advancing related technologies. In the present work, the issue of limited FOV of digital holography was explored, and the FOV was doubled by employing a very simple and affordable optical component. A cube beam splitter, strategically oriented at ∼45° w.r.t. the optical axis is placed in the object beam, which helps to create a multiplexed hologram, carrying double object information. The double-FOV digital holography represents a significant advancement in the study of transparent objects, offering enhanced capabilities in imaging and analysis. This technique overcomes traditional limitations associated with conventional digital holography by providing simultaneous access to both FOVs. The major advantage of the proposed system is its simple optical layout by using a simple and affordable optical component. The experimentally obtained results on various transparent objects corroborate the imaging and optical measurement capability of the system. This approach is crucial for detailed examinations of transparent structures, such as biological samples or microfluidic devices, where capturing details with larger context is essential for comprehensive analysis. By integrating multiple views into a single holographic frame, researchers can achieve a more complete understanding of the three-dimensional morphology and dynamic behavior of transparent specimens. Further, it achieves high bandwidth imaging with an enhanced space bandwidth utilization of 19.63%. The quantitative assessment of the reconstructed images is provided by measuring the signal-to-noise ratio (SNR). The measured SNR values for the reconstructed images [Figure 2a,d] are 12.15 and 12.38, respectively. Challenges remain, including the lower temporal stability and lateral resolution with the proposed system. The lateral resolution and temporal stability achieved by the proposed system are 12.40 µm and 0.189 radians, respectively. However, the resolution of the system is marginally lower than a conventional single-channel digital holography due to the multiplexing [27]. Also, in comparison to a common-path digital holographic system, the temporal stability is lower due to the double-channel Mach–Zehnder-type optical layout. The alignment of multiple optical paths and the synchronization of recording planes require meticulous calibration to ensure accurate reconstruction and interpretation of holographic data. However, ongoing advancements continue to address these challenges,

expanding the practicality and applicability of the proposed system in diverse research and industrial settings.

Overall, the double-FOV digital holography represents a transformative approach to studying transparent objects, offering unprecedented capabilities in imaging, analysis, and real-time monitoring across multiple spatial scales. As research and technology continue to evolve, the system holds promise for unlocking new insights into the intricate structures and dynamic behaviors of transparent materials and biological specimens alike.

5. Conclusions

The continual evolution of optical metrology has led to remarkable strides in high-bandwidth digital holography, particularly for the analysis of transparent objects where traditional measurement techniques often fall short. This article has explored the limitations of conventional digital holography, especially in terms of FOV. In this work, the double FOV is achieved by employing a cube beam splitter in the object beam with an orientation of $\sim 45^{\circ}$ with respect to the optical axis, which strategically folds the two distinct FOVs onto the active area of the image sensor. Therefore, this configuration enables the recording of two different areas of the object in a single shot, hence extending the FOV by double that of a digital holographic system. The proof of the concept is experimentally demonstrated on different objects. Further, some optical metrological applications are experimentally demonstrated by performing experiments for measuring the glass plate thickness and phase imaging of candle flame with double FOV. Therefore, this digital holographic system, leveraging single-shot double-FOV capability, can effectively be used for the analysis of scientific and industrial measurement applications.

Through the advancement of developing a single-shot double-FOV configuration, digital holography has transitioned from a laboratory tool to a versatile, high-precision imaging modality. This method has enabled real-time, non-invasive optical measurement applications, including surface profiling, temperature mapping, and refractive index profiling in transparent media with improved object information.

Author Contributions: Conceptualization, M.K.; methodology, M.K. and L.P.; software, M.K., L.P. and K.K.; validation, M.K., L.P., K.K., R.K., Y.A. and O.M.; formal analysis, M.K.; investigation, M.K., L.P., K.K., R.K., Y.A. and O.M.; data curation, M.K.; writing—original draft preparation, M.K.; writing—review and editing, M.K., L.P., K.K., R.K., Y.A. and O.M.; visualization, M.K., L.P., K.K., R.K., Y.A. and O.M.; supervision, M.K. and O.M.; project administration, M.K., Y.A. and O.M.; funding acquisition, M.K., Y.A. and O.M. All authors have read and agreed to the published version of the manuscript.

Funding: This research was funded by ANRF, grant number RJF/2023/000048.

Institutional Review Board Statement: Not applicable.

Informed Consent Statement: Not applicable.

Data Availability Statement: Data underlying the results presented in this paper are not publicly available at this time but may be obtained from the authors upon reasonable request.

Conflicts of Interest: The authors declare no conflicts of interest.

References

1. Santiago, J.G.; Wereley, S.T.; Meinhart, C.D.; Beebe, D.J.; Adrian, R.J. A Particle Image Velocimetry System for Microfluidics. *Exp. Fluids* **1998**, *25*, 316–319. [CrossRef]
2. Docquier, N.; Candel, S. Combustion Control and Sensors: A Review. *Prog. Energy Combust. Sci.* **2002**, *28*, 107–150. [CrossRef]
3. Wang, L.V.; Hu, S. Photoacoustic Tomography: In Vivo Imaging from Organelles to Organs. *Science* **2012**, *335*, 1458–1462. [CrossRef] [PubMed]

4. Song, G.; Wang, Y.; Tan, D.Q. A Review of Surface Roughness Impact on Dielectric Film Properties. *IET Nanodielectrics* **2022**, *5*, 1–23. [CrossRef]
5. Zhang, K.; Choi, S.; Sasaki, O.; Luo, S.; Suzuki, T.; Liu, Y.; Pu, J. Large Thickness Measurement of Glass Plates with a Spectrally Resolved Interferometer Using Variable Signal Positions. *OSA Contin.* **2021**, *4*, 1792. [CrossRef]
6. Kumar, Y.P.; Chatterjee, S. Thickness Measurement of Transparent Glass Plates Using a Lateral Shearing Cyclic Path Optical Configuration Setup and Polarization Phase Shifting Interferometry. *Appl. Opt.* **2010**, *49*, 6552. [CrossRef]
7. Kim, S.; Kim, Y.; Shin, S.-C.; Hibino, K.; Sugita, N. Interferometric Thickness Measurement of Glass Plate by Phase-Shifting Analysis Using Wavelength Scanning with Elimination of Bias Phase Error. *Opt. Rev.* **2021**, *28*, 48–57. [CrossRef]
8. Omega Engineering. *Temperature Measurement Handbook*; Omega Press: New Lebanon, NY, USA, 1995.
9. Maldague, X.P. *Theory and Practice of Infrared Technology for Nondestructive Testing*; Wiley Series in Microwave and Optical Engineering; Wiley: New York, NY, USA, 2001; ISBN 978-0-471-18190-3.
10. Hariharan, P. *Optical Interferometry*; Elsevier: Amsterdam, The Netherlands, 2003; ISBN 978-0-12-311630-7.
11. Schnars, U.; Jüptner, W. Direct Recording of Holograms by a CCD Target and Numerical Reconstruction. *Appl. Opt.* **1994**, *33*, 179. [CrossRef]
12. Sheridan, J.T.; Kostuk, R.K.; Gil, A.F.; Wang, Y.; Lu, W.; Zhong, H.; Tomita, Y.; Neipp, C.; Francés, J.; Gallego, S.; et al. Roadmap on Holography. *J. Opt.* **2020**, *22*, 123002. [CrossRef]
13. Kreis, T.M. Frequency Analysis of Digital Holography. *Opt. Eng.* **2002**, *41*, 771. [CrossRef]
14. Shaked, N.T.; Katz, B.; Rosen, J. Review of Three-Dimensional Holographic Imaging by Multiple-Viewpoint-Projection Based Methods. *Appl. Opt.* **2009**, *48*, H120. [CrossRef] [PubMed]
15. Stępień, P.; Korbuszewski, D.; Kujawińska, M. Digital Holographic Microscopy with Extended Field of View Using Tool for Generic Image Stitching. *ETRI J.* **2019**, *41*, 73–83. [CrossRef]
16. Di, J.; Zhao, J.; Jiang, H.; Zhang, P.; Fan, Q.; Sun, W. High Resolution Digital Holographic Microscopy with a Wide Field of View Based on a Synthetic Aperture Technique and Use of Linear CCD Scanning. *Appl. Opt.* **2008**, *47*, 5654. [CrossRef] [PubMed]
17. Sha, B.; Liu, X.; Ge, X.-L.; Guo, C.-S. Fast Reconstruction of Off-Axis Digital Holograms Based on Digital Spatial Multiplexing. *Opt. Express* **2014**, *22*, 23066. [CrossRef]
18. Girshovitz, P.; Shaked, N.T. Doubling the Field of View in Off-Axis Low-Coherence Interferometric Imaging. *Light Sci. Appl.* **2014**, *3*, e151. [CrossRef]
19. Shaked, N.T.; Micó, V.; Trusiak, M.; Kuś, A.; Mirsky, S.K. Off-Axis Digital Holographic Multiplexing for Rapid Wavefront Acquisition and Processing. *Adv. Opt. Photon.* **2020**, *12*, 556. [CrossRef]
20. Rubin, M.; Dardikman, G.; Mirsky, S.K.; Turko, N.A.; Shaked, N.T. Six-Pack off-Axis Holography. *Opt. Lett.* **2017**, *42*, 4611. [CrossRef]
21. Tayebi, B.; Sharif, F.; Jafarfard, M.R.; Kim, D.Y. Double-Field-of-View, Quasi-Common-Path Interferometer Using Fourier Domain Multiplexing. *Opt. Express* **2015**, *23*, 26825. [CrossRef]
22. Tayebi, B.; Kim, W.; Yoon, B.-J.; Han, J.-H. Real-Time Triple Field of View Interferometry for Scan-Free Monitoring of Multiple Objects. *IEEE/ASME Trans. Mechatron.* **2018**, *23*, 160–166. [CrossRef]
23. Zhang, W.; Cao, L.; Jin, G.; Brady, D. Full Field-of-View Digital Lens-Free Holography for Weak-Scattering Objects Based on Grating Modulation. *Appl. Opt.* **2018**, *57*, A164. [CrossRef]
24. Lee, B.; Jang, C.; Kim, D.; Lee, B. Single Grating Reflective Digital Holography With Double Field of View. *IEEE Trans. Ind. Inf.* **2019**, *15*, 6155–6161. [CrossRef]
25. Kumar, M.; Pensia, L.; Kumar, R. Single-Shot off-Axis Digital Holographic System with Extended Field-of-View by Using Multiplexing Method. *Sci. Rep.* **2022**, *12*, 16462. [CrossRef] [PubMed]
26. Pensia, L.; Kumar, M.; Kumar, R. Dual Field-of-View Off-Axis Spatially Multiplexed Digital Holography Using Fresnel's Bi-Mirror. *Sensors* **2024**, *24*, 731. [CrossRef] [PubMed]
27. Kumar, M.; Yoneda, N.; Pensia, L.; Muniraj, I.; Anand, V.; Kumar, R.; Murata, T.; Awatsuji, Y.; Matoba, O. Light Origami Multi-Beam Interference Digital Holographic Microscope for Live Cell Imaging. *Opt. Laser Technol.* **2024**, *176*, 110961. [CrossRef]
28. Kumar, M.; Murata, T.; Matoba, O. Double Field-of-View Single-Shot Common-Path off-Axis Reflective Digital Holographic Microscope. *Appl. Phys. Lett.* **2023**, *123*, 223702. [CrossRef]
29. Pensia, L.; Kumar, M.; Kumar, R. A Compact Digital Holographic System Based on a Multifunctional Holographic Optical Element with Improved Resolution and Field of View. *Opt. Lasers Eng.* **2023**, *169*, 107744. [CrossRef]
30. Kumar, M.; Matoba, O. 2D Full-Field Displacement and Vibration Measurements of Specularly Reflecting Surfaces by Two-Beam Common-Path Digital Holography. *Opt. Lett.* **2021**, *46*, 5966. [CrossRef]
31. Kumar, M.; Pensia, L.; Kumar, R.; Matoba, O. Lensless Fourier Transform Multiplexed Digital Holography. *Opt. Lett.* **2025**, *50*, 1909. [CrossRef]
32. Kumar, M.; Pensia, L.; Kumar, R.; Matoba, O. Vibration Measurement of 3-D Objects With Single-Shot Double Field-of-View High-Speed Digital Holography. *IEEE Trans. Instrum. Meas.* **2025**, *74*, 4507408. [CrossRef]

33. Pensia, L.; Kumar, M.; Matoba, O.; Kumar, R. Enhancing Field of View of Digital Holography Using an Angular Multiplexed Holographic Optical Element. *Opt. Lett.* **2025**, *50*, 3970. [CrossRef]
34. Ji, J.; Xie, H.; Yang, L. Learned Large Field-of-View Imager with a Simple Spherical Optical Module. *Opt. Commun.* **2023**, *526*, 128918. [CrossRef]
35. Huang, Z.; Cao, L. High Bandwidth-Utilization Digital Holographic Multiplexing: An Approach Using Kramers–Kronig Relations. *Adv. Photonics Res.* **2022**, *3*, 2100273. [CrossRef]
36. Mundt, J.; Kreis, T.M. Digital Holographic Recording and Reconstruction of Large Scale Objects for Metrology and Display. *Opt. Eng.* **2010**, *49*, 125801. [CrossRef]
37. Kumar, R.; Dwivedi, G.; Singh, O. Portable Digital Holographic Camera Featuring Enhanced Field of View and Reduced Exposure Time. *Opt. Lasers Eng.* **2021**, *137*, 106359. [CrossRef]
38. Kim, K.; Jung, J.; Kim, C.; Ahn, G.; Kim, Y.-J. AI-Driven Pseudo-Light Source for Achieving High Coherence and Low Speckle Noise Simultaneously in Dual-Wavelength Digital Holographic Microscopy. *Opt. Laser Technol.* **2025**, *181*, 111572. [CrossRef]
39. Settles, G.S.; Hargather, M.J. A Review of Recent Developments in Schlieren and Shadowgraph Techniques. *Meas. Sci. Technol.* **2017**, *28*, 042001. [CrossRef]
40. Sweeney, D.W.; Vest, C.M. Measurement of Three-Dimensional Temperature Fields above Heated Surfaces by Holographic Interferometry. *Int. J. Heat Mass Transf.* **1974**, *17*, 1443–1454. [CrossRef]
41. Farrell, P.V.; Springer, G.S.; Vest, C.M. Heterodyne Holographic Interferometry: Concentration and Temperature Measurements in Gas Mixtures. *Appl. Opt.* **1982**, *21*, 1624. [CrossRef]
42. Reuss, D.L. Temperature Measurements in a Radially Symmetric Flame Using Holographic Interferometry. *Combust. Flame* **1983**, *49*, 207–219. [CrossRef]
43. Keren, E.; Bar-Ziv, E.; Glatt, I.; Kafri, O. Measurements of Temperature Distribution of Flames by Moire Deflectometry. *Appl. Opt.* **1981**, *20*, 4263. [CrossRef]
44. Farrell, P.V.; Hofeldt, D.L. Temperature Measurement in Gases Using Speckle Photography. *Appl. Opt.* **1984**, *23*, 1055. [CrossRef] [PubMed]
45. Stella, A.; Guj, G.; Giammartini, S. Measurement of Axisymmetric Temperature Fields Using Reference Beam and Shearing Interferometry for Application to Flames. *Exp. Fluids* **2000**, *29*, 1–12. [CrossRef]
46. Kumar, M.; Shakher, C. Measurement of Temperature and Temperature Distribution in Gaseous Flames by Digital Speckle Pattern Shearing Interferometry Using Holographic Optical Element. *Opt. Lasers Eng.* **2015**, *73*, 33–39. [CrossRef]
47. Kumar, M.; Agarwal, S.; Kumar, V.; Khan, G.S.; Shakher, C. Experimental Investigation on Butane Diffusion Flames under the Influence of Magnetic Field by Using Digital Speckle Pattern Interferometry. *Appl. Opt.* **2015**, *54*, 2450. [CrossRef]
48. Doleček, R.; Psota, P.; Lédl, V.; Vít, T.; Václavík, J.; Kopecký, V. General Temperature Field Measurement by Digital Holography. *Appl. Opt.* **2013**, *52*, A319. [CrossRef]
49. Guerrero-Mendez, C.; Anaya, T.S.; Araiza-Esquivel, M.; Balderas-Navarro, R.E.; Aranda-Espinoza, S.; López-Martínez, A.; Olvera-Olvera, C. Real-Time Measurement of the Average Temperature Profiles in Liquid Cooling Using Digital Holographic Interferometry. *Opt. Eng.* **2016**, *55*, 121730. [CrossRef]
50. Kumar, M.; Matoba, O.; Quan, X.; Rajput, S.K.; Awatsuji, Y.; Tamada, Y. Single-Shot Common-Path off-Axis Digital Holography: Applications in Bioimaging and Optical Metrology [Invited]. *Appl. Opt.* **2021**, *60*, A195. [CrossRef]
51. Kumon, Y.; Hashimoto, S.; Inoue, T.; Nishio, K.; Kumar, M.; Matoba, O.; Xia, P.; Rajput, S.K.; Awatsuji, Y. Three-Dimensional Video Imaging of Dynamic Temperature Field of Transparent Objects Recorded by a Single-View Parallel Phase-Shifting Digital Holography. *Opt. Laser Technol.* **2023**, *167*, 109808. [CrossRef]
52. Xia, P.; Ri, S.; Inoue, T.; Awatsuji, Y.; Matoba, O. Three-Dimensional Dynamic Measurement of Unstable Temperature Fields by Multi-View Single-Shot Phase-Shifting Digital Holography. *Opt. Express* **2022**, *30*, 37760. [CrossRef]
53. Dardikman, G.; Shaked, N.T. Is Multiplexed Off-Axis Holography for Quantitative Phase Imaging More Spatial Bandwidth-Efficient than on-Axis Holography? [Invited]. *J. Opt. Soc. Am. A* **2019**, *36*, A1. [CrossRef]
54. Bioucas-Dias, J.M.; Valadao, G. Phase Unwrapping via Graph Cuts. *IEEE Trans. Image Process.* **2007**, *16*, 698–709. [CrossRef]

Disclaimer/Publisher's Note: The statements, opinions and data contained in all publications are solely those of the individual author(s) and contributor(s) and not of MDPI and/or the editor(s). MDPI and/or the editor(s) disclaim responsibility for any injury to people or property resulting from any ideas, methods, instructions or products referred to in the content.